

## Supplementary Items Summary

### Supplementary Figures

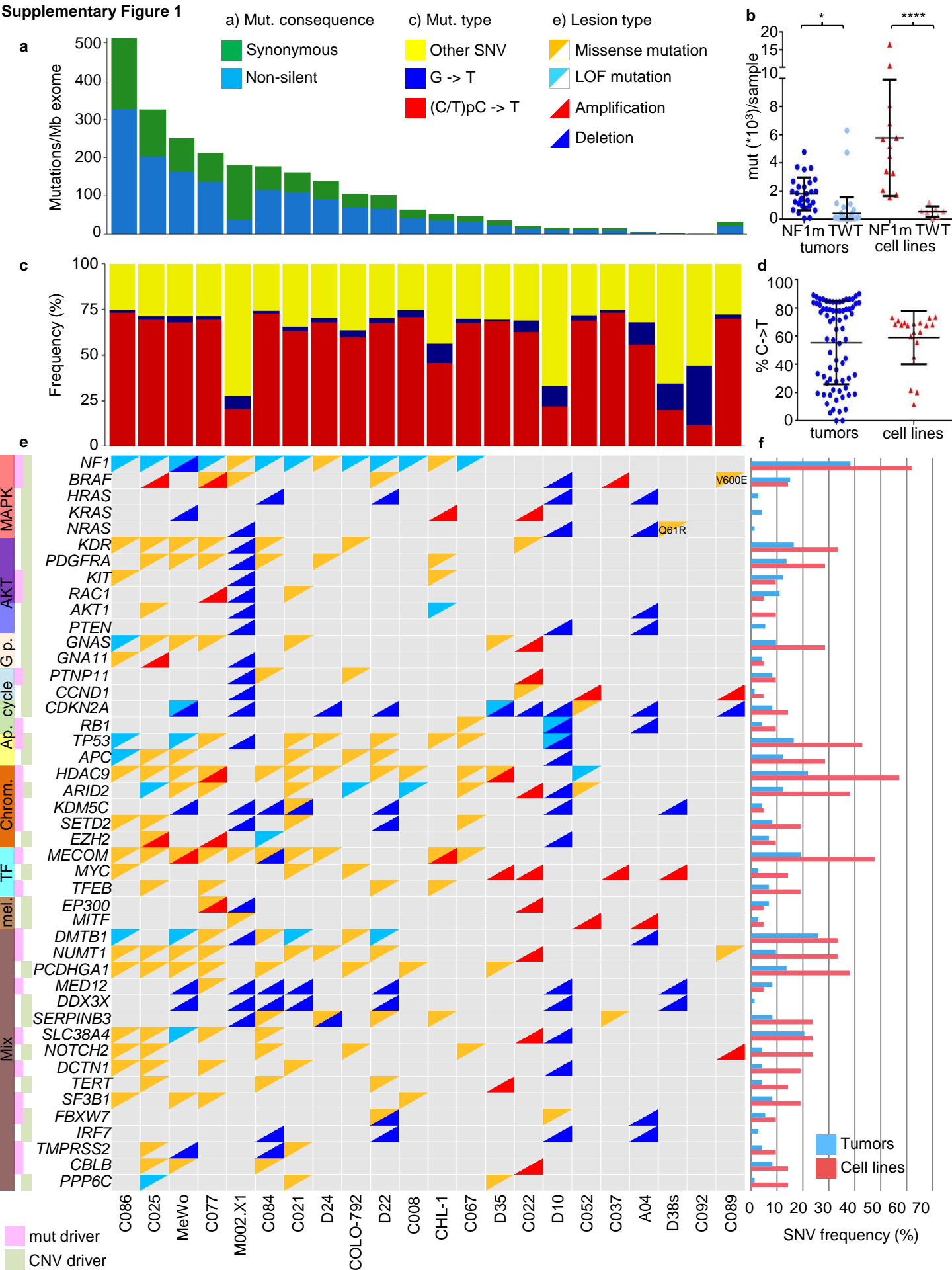
- Supplementary Figure 1. Landscape of the alterations and drug sensitivity in the collection of 22 melanoma cell lines. (Panels a-j, PDF file)
- Supplementary Figure 2. Clonogenic assays confirmed the synergy of temozolomide with olaparib and nilotinib with MEK inhibitors. (Panels a-b, PDF file)
- Supplementary Figure 3. Identification of the association between AXL expression and synergy between trametinib and nilotinib. (Panels a-l, PDF file)
- Supplementary Figure 4. Identification of trametinib and nilotinib/trametinib drug resistance genes by CRISPR/Cas9 genome-wide library screening. (Panels a-q, PDF file).

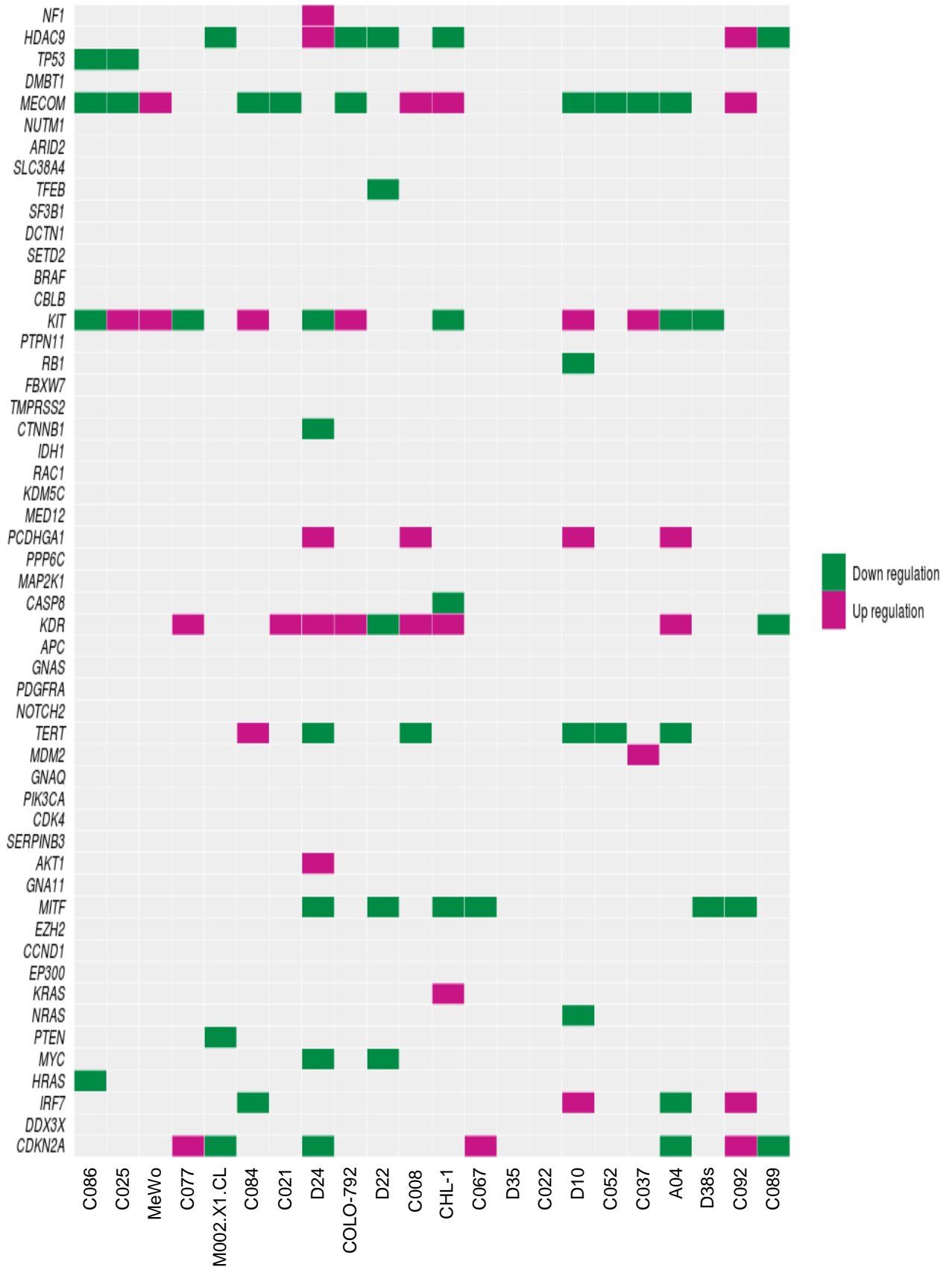
### Supplementary Tables

- Supplementary Table 1. Summary of the data available for each cell line. (Sheets a-b; Excel file)
- Supplementary Table 2. Somatic single nucleotide mutation in the collection of 22 melanoma cell lines. (Sheets a-c, Excel file)
- Supplementary Table 3. Copy number variation data for the 22 cell lines used in the screening. (Sheets a-b, Excel file)
- Supplementary Table 4. Gene expression data for the cell lines used in the high-throughput drug screening. (Sheets a-c, Excel file)
- Supplementary Table 5. MicroRNA expression data for the cell lines used in the high-throughput drug screening. (Sheets a-c, excel file)
- Supplementary Table 6. Validation of somatic single nucleotide mutation by RNA sequencing data analysis. (one sheet, Excel file)
- Supplementary Table 7. Definition of the *BRAF/NRAS* WT melanoma driver genes and driver mutations. (Sheets a-d, Excel file)
- Supplementary Table 8. Description of the drugs used for the high-throughput screening. (one sheet; Excel file)
- Supplementary Table 9. Results of the high-throughput drug screening. (Sheets a-e, Excel file)
- Supplementary Table 10. Results of the low throughput viability assays for the validation of the drug combination synergies. (Sheets a-d, Excel file)
- Supplementary Table 11. Results from the biological replicates of the low-throughput validation assays. (Sheets a-b, Excel file)
- Supplementary Table 12. Cell line lesions used for the association analysis with drug synergy. (Sheets a-b, Excel file)
- Supplementary Table 13. Results of the statistical analyses performed to identify associations between lesions and drug synergy. (Sheets a-d, Excel file)
- Supplementary Table 14. Genes differentially expressed between cell lines that are sensitive or non-sensitive to nilotinib/trametinib combination. (Sheets a-d, Excel file)
- Supplementary Table 15. MITF and AXL expression levels and their association with the synergy between nilotinib and trametinib. (Sheets a-c, Excel file)
- Supplementary Table 16. Effects of AXL overexpression and knockdown on the synergy between nilotinib and trametinib. (one sheet; Excel file)

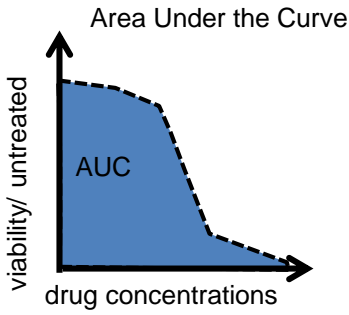
- Supplementary Table 17. Phosphoproteome analysis of a sensitive and a non-sensitive cell line treated with nilotinib, trametinib or nilotinib/trametinib combination. (Sheets A-c, Excel file)
- Supplementary Table 18. Nilotinib/trametinib combination resistance genes identified by CRISPR/Cas9 screens. (Sheets a-k, Excel file)
- Supplementary Table 19. Trametinib resistance genes identified by CRISPR/Cas9 screens. (Sheets a-j, Excel file)
- Supplementary Table 20. Pathway enrichment analysis for the genes whose loss confer resistance to trametinib or nilotinib/trametinib combination in each cell line. (Sheets a-h, Excel file)
- Supplementary Table 21. Pathway enrichment analysis for the genes that confer resistance to trametinib or nilotinib/trametinib combination in 2 or more cell lines. (Sheets a-b, Excel file)

Supplementary Figure 1

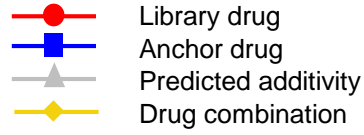




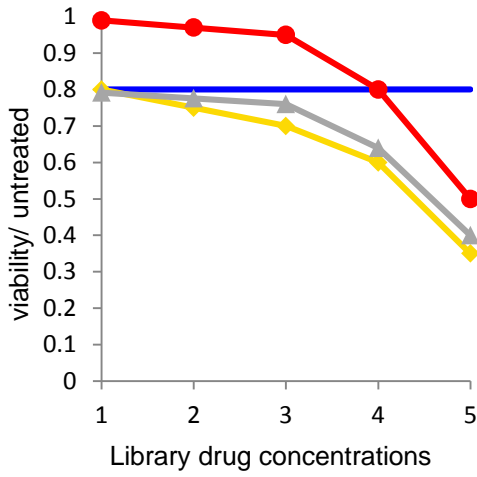
h



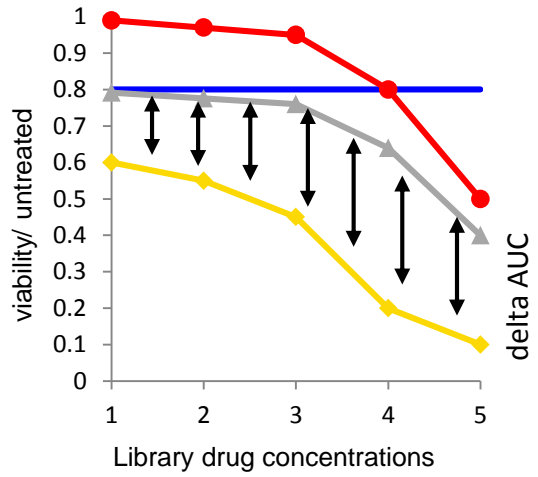
Legend a and c



Additive effect



Synergy



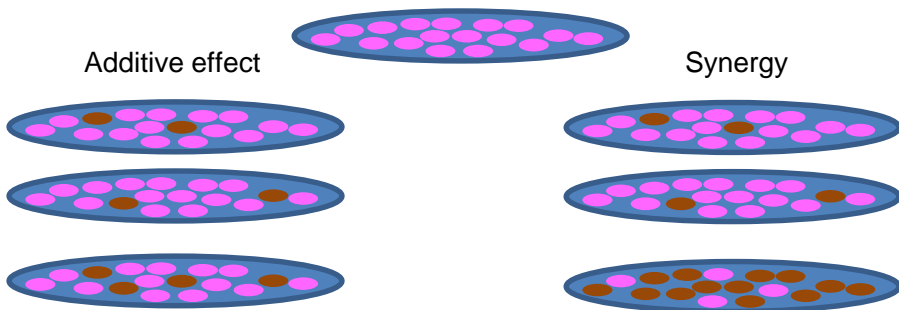
Additive effect

Synergy

Drug 1

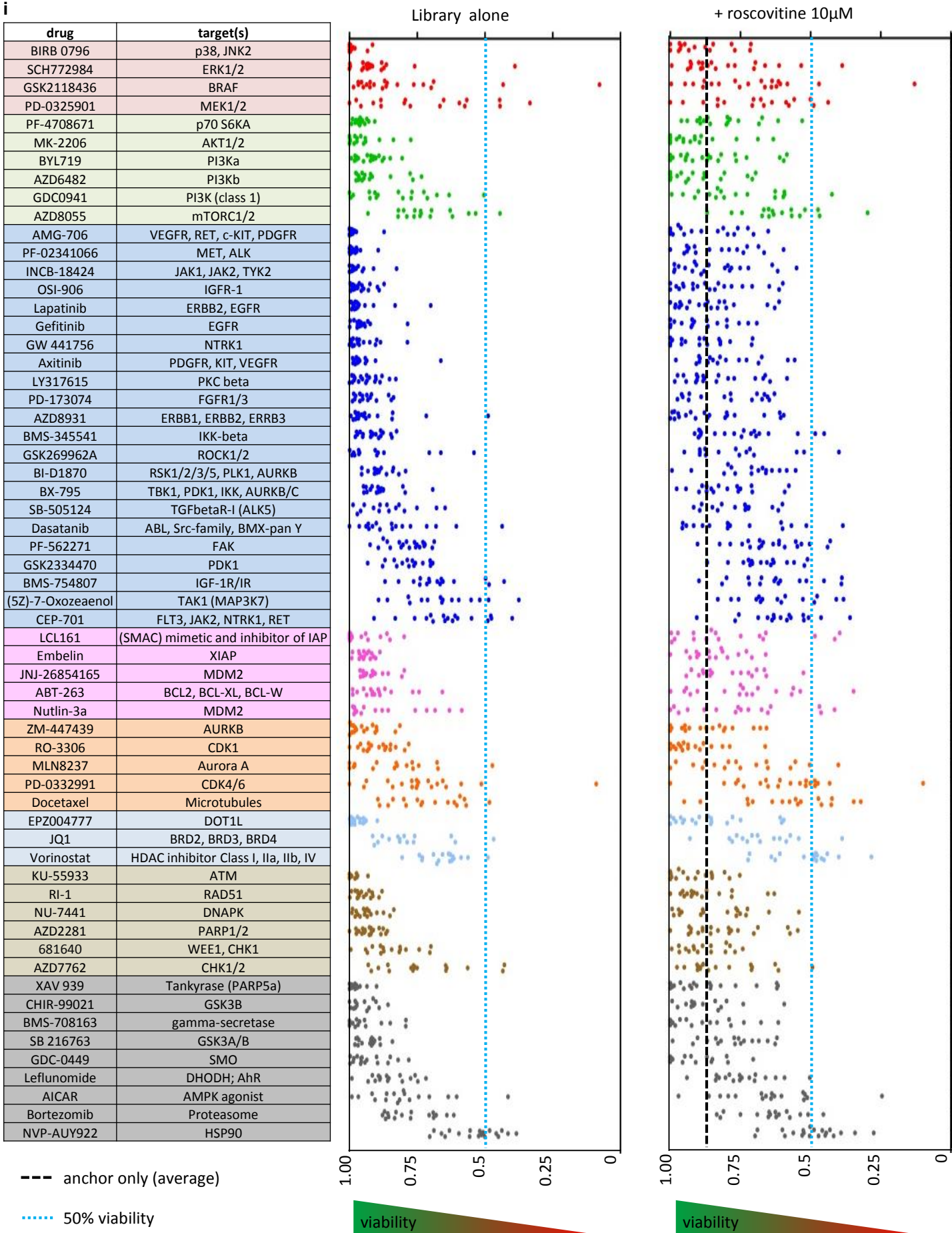
Drug 2

Drug 1+2



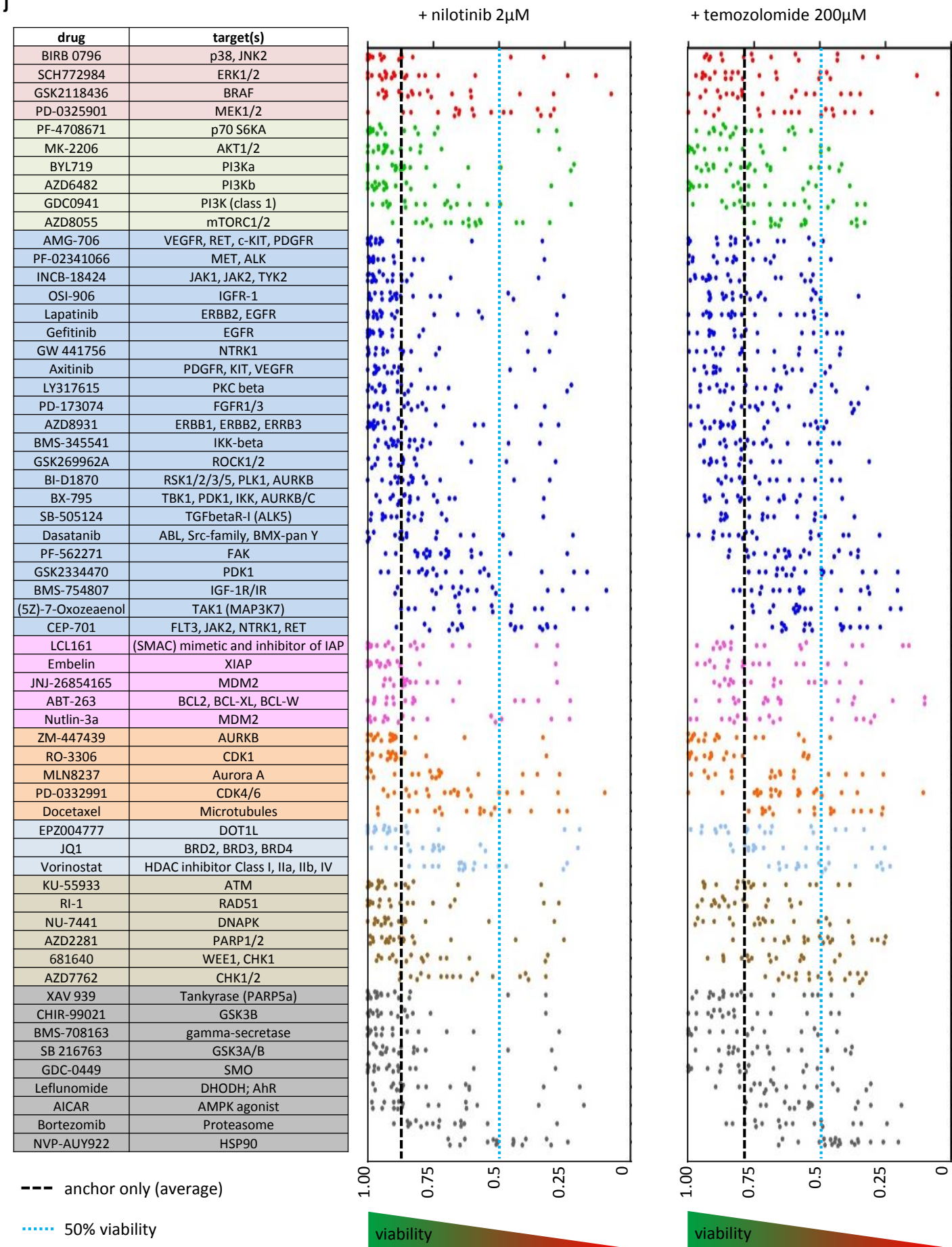
Supplementary Figure 1

i



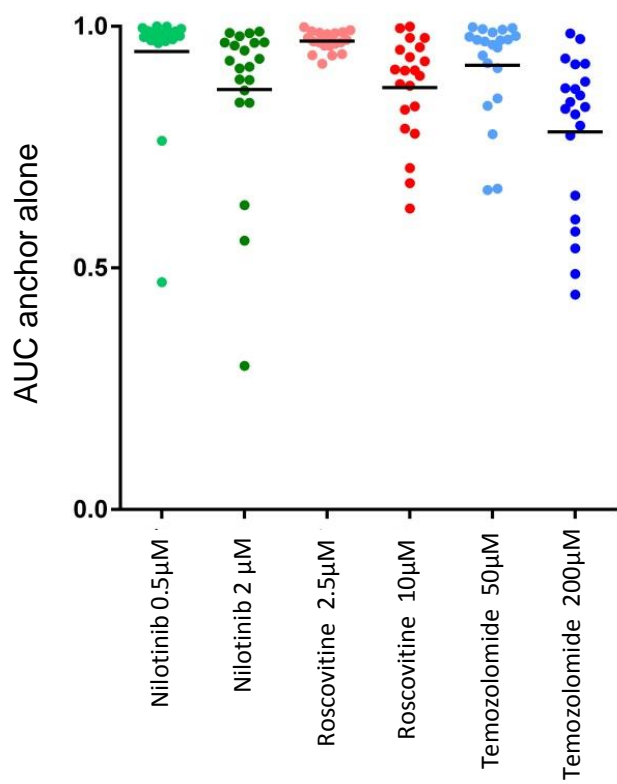
Supplementary Figure 1

j



k

AUC anchor alone



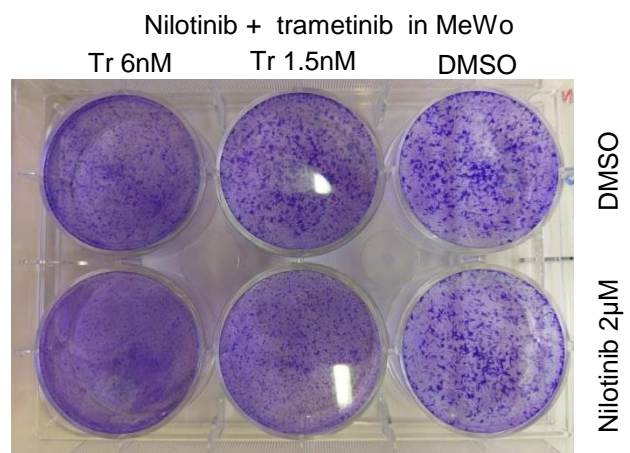
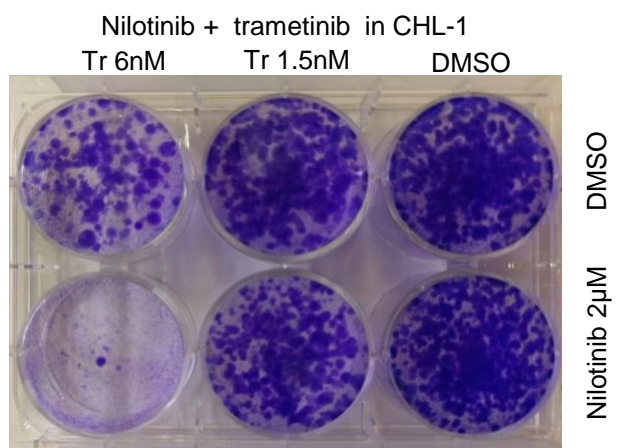
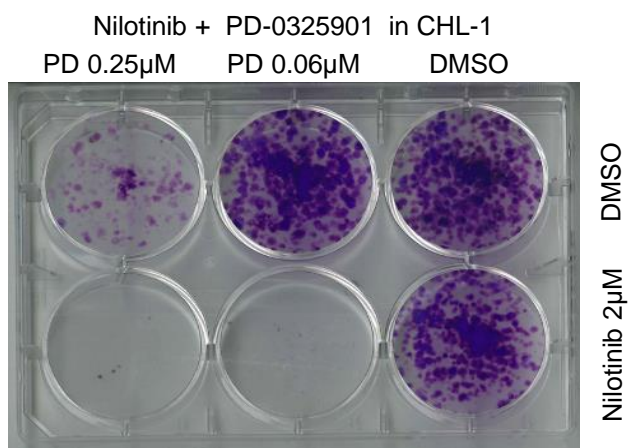
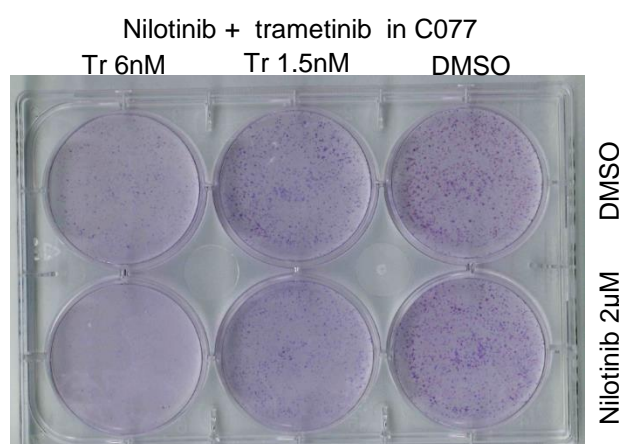
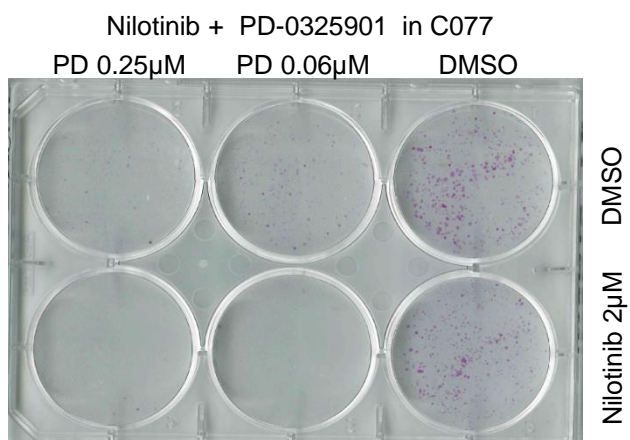
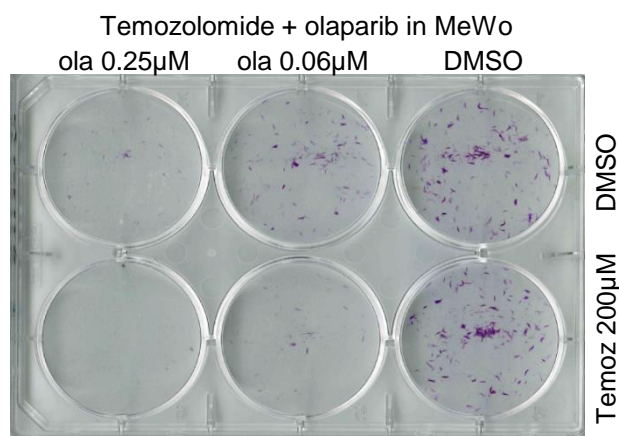
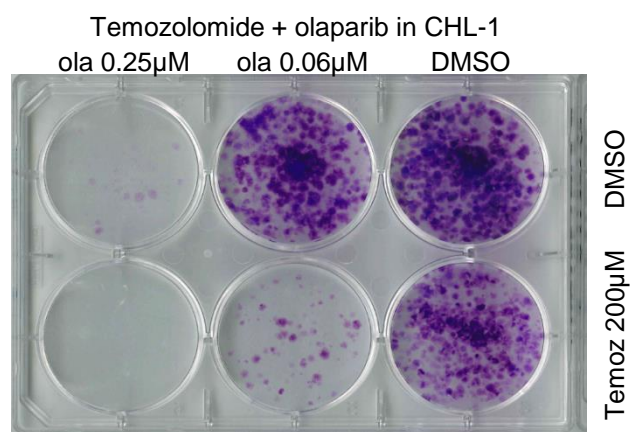


## Supplementary Figure 1. Landscape of the alterations and drug sensitivity in the collection of 22 melanoma cell lines.

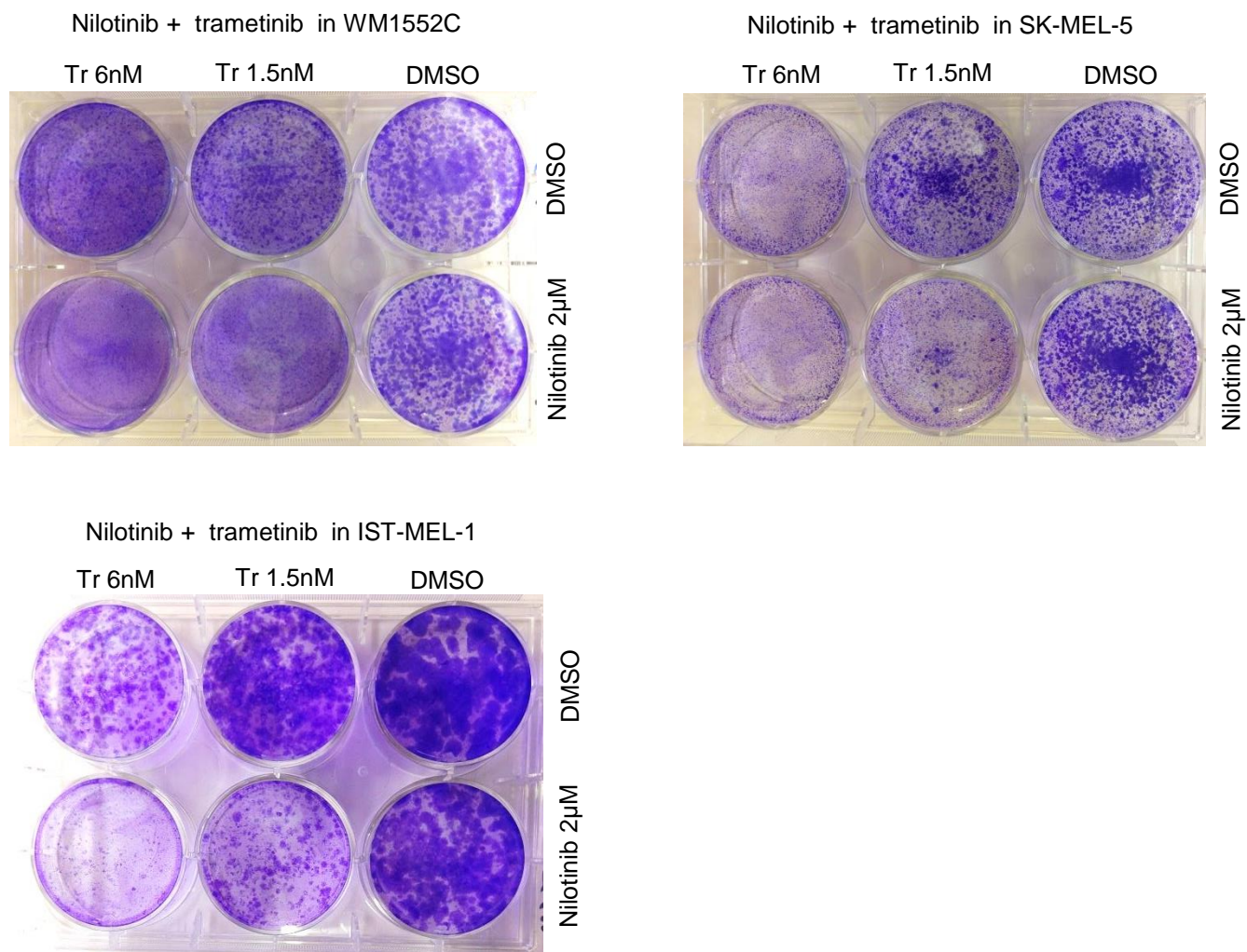
**a)** Frequency of somatic mutation (see **Methods**) per Mb of exome in each of the 22 melanoma cell lines; cell line ID at the bottom of the page. **b)** Frequency of mutations in *NFI* mutant (NF1m) and triple wild type (TWT) cell lines (right 2 columns) and human tumors (left 2 columns). Y axis represents the number (in thousands) of mutations per sample, mean and standard deviation are shown. Significance by one way Anova and Tukey's multiple comparison test. \* = $P<0.05$ ; \*\*\*\*  $P<0.0001$ . **c)** Frequency (%) of mutation spectra, legend at the top of the page. **d)** C to T at dipyrimidines frequency in *BRAF/NRAS* wild type melanoma cell lines (red) and tumors (blue); mean and standard deviation are shown. **e)** Status of the melanoma drivers, legend at the top of the page. If both missense and LOF mutation occurs in a gene, LOF was displayed. Gene symbol is displayed on the left; grey and pink indicate if the gene is a copy number variation driver (CNV driver) or a *BRAF/NRAS* WT melanoma mutation driver, respectively (see **Methods**). Genes were grouped in main functional families with different color code, from top: MAPK, AKT, G protein (G p.), cell cycle (cycle), apoptosis (Ap.), Chromatin remodelling (Chrom.), transcription factors (TF), melanoma pigmentation (Mel), mixed function (Mix). Only genes mutated in 3 or more cell lines are displayed. C089 and D38s carry hotspot mutations in *BRAF* and *NRAS* as indicated by the amino acid code. **f)** Frequency of *BRAF/NRAS* wild type melanoma cell lines (red) or tumors (pale blue) with a single nucleotide mutation in the melanoma driver genes displayed on the left. **g)** Approach to estimate drug synergy (see **Methods**). We calculated the area under the viability curve (AUC) for each treatment (top left), then the predicted additivity as arithmetic product of the viability of the cells treated with anchor and the library drug alone, and then calculated the delta AUC as AUC of the predicted additivity minus the AUC of the drug combination. An additive combination (yellow line, left panel) results in a growth inhibition that is the sum of the 2 single drugs (grey line, left panel), while a synergistic combination (yellow line, right panel) displays a growth inhibition much higher than the predicted additivity (grey line, right panel), thus scoring a positive delta AUC (double arrows area). An outline of the growth inhibition effects is displayed in the bottom panel, where pink circles represent viable cells, brown circles represent dead cells. **h-i)** Viability of the cell lines treated with 60 library drugs (left panel in i) or 180 drug combinations (right panel in i, left and right panel in j). Each dot represents the AUC (on the X axis) of a cell line treated with a library drug or its combination with the anchor drug (on top of the panel). Each row represents a library drug in colour code according to the molecular pathway/function of the main drug target, from top: MAPK, AKT, other kinases, apoptosis, cell cycle, chromatin remodelling, DNA replication, other function. The dotted blue line highlights 50% growth inhibition, the dashed black line shows the AUC of the anchor drug alone. The table on the left describes each library drug and its putative target(s). **j)** AUC (Y axis) of the cell line treated with 2 concentrations the anchor drugs alone (X axis). The black line shows the mean.

# Supplementary Figure 2

a



b

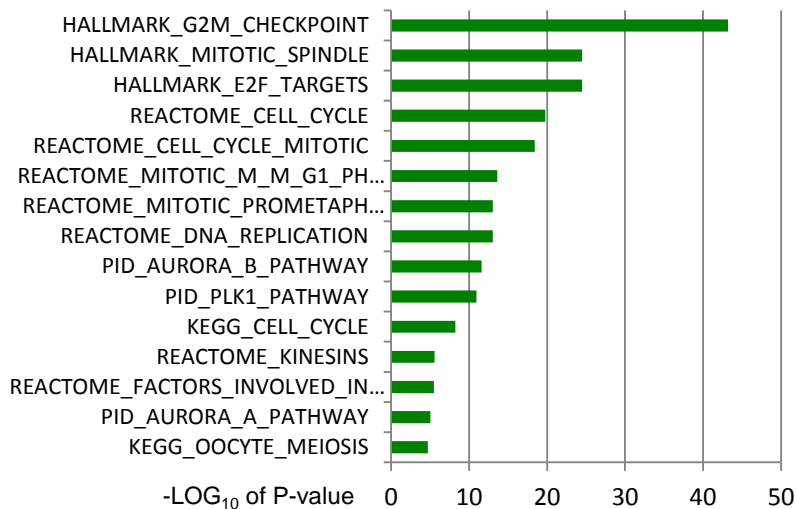


**Supplementary Figure 2. Clonogenic assays confirmed the synergy of temozolomide with olaparib and nilotinib with MEK inhibitors.**

a) Clonogenic assays (2 weeks) of representative *BRAF/NRAS* wild type melanoma cell lines. b) Clonogenic assays of representative *BRAF<sup>V600</sup>*-mutant cell lines. The concentrations of the library and anchor drugs are indicated on the top or on the right, respectively.

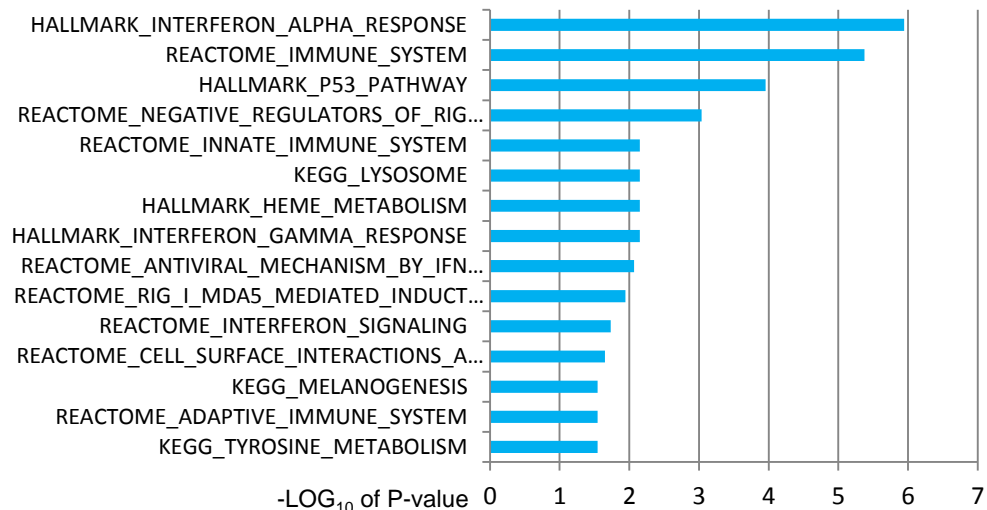
**a**

up-regulated genes



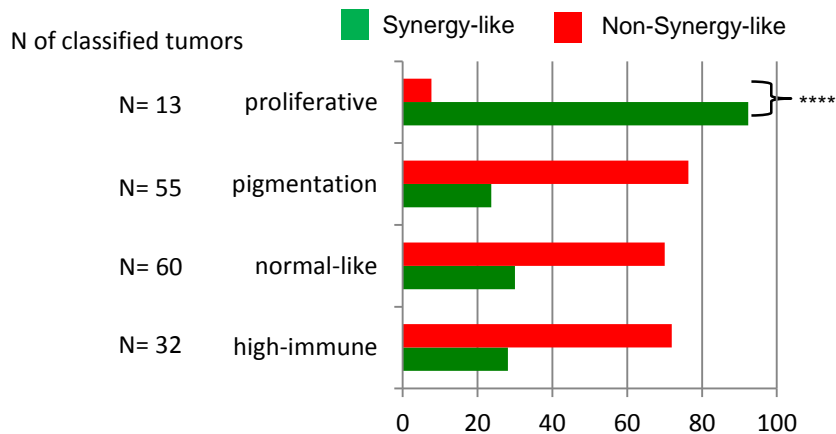
**b**

Down-regulated genes



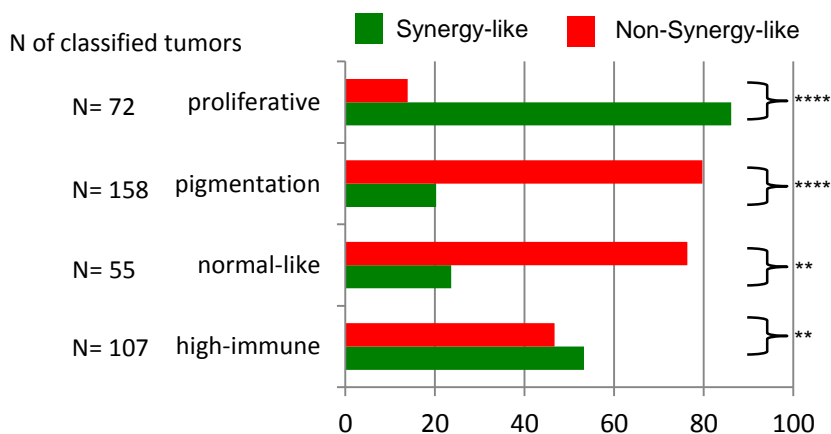
**c**

**Leeds' cohort** n= 208  
 Synergy-like n=55 (26.4%)  
 Non-synergy-like n=110 (52.9%)  
 Unclassified n=43 (20.7%)

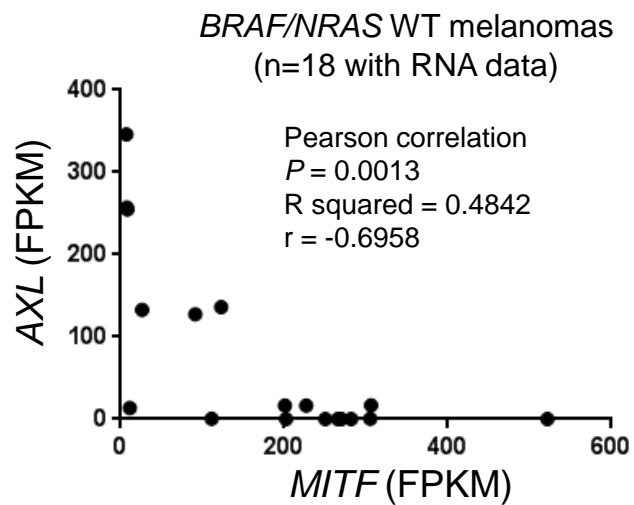


**d**

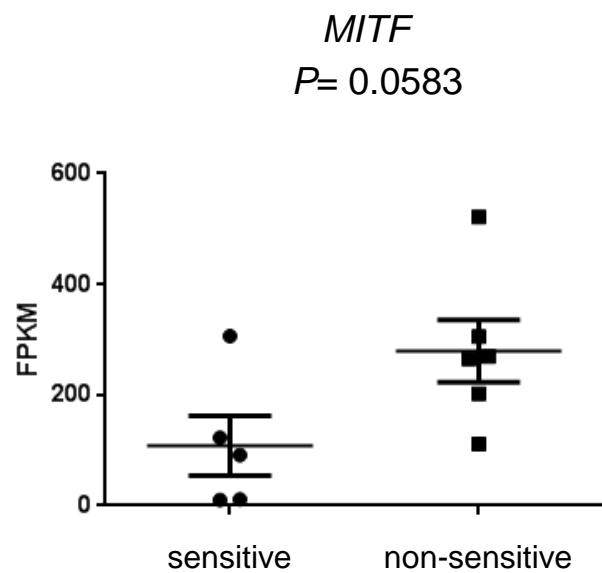
**TCGA cohort** n= 474  
 Synergy-like n=164 (34.6%)  
 Non-synergy-like n=242 (51.1%)  
 Unclassified n=68 (14.3%)



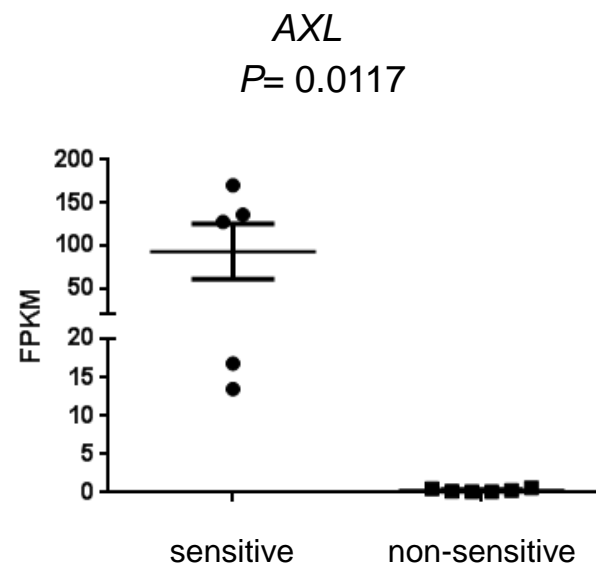
e



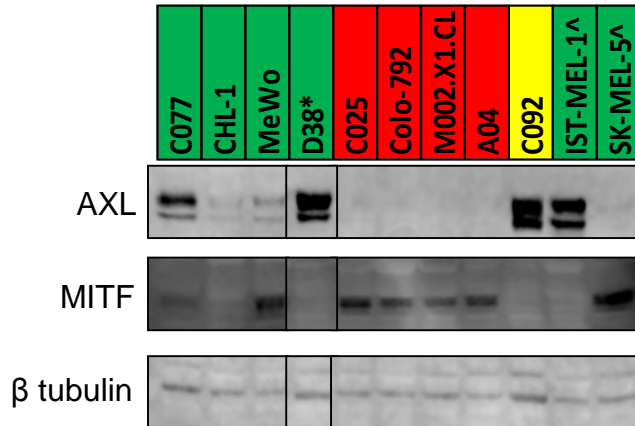
f



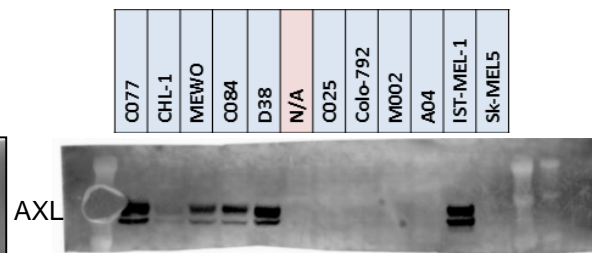
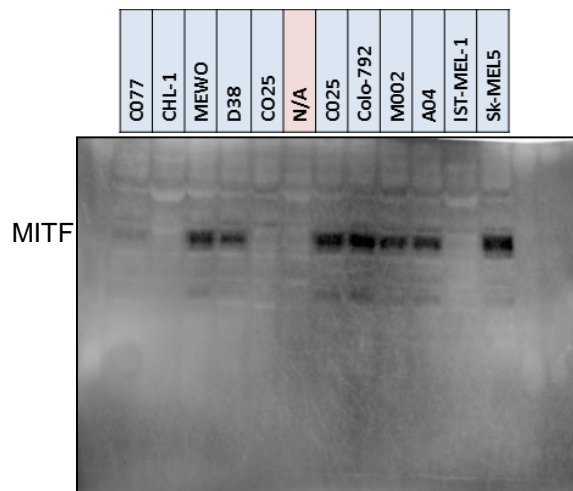
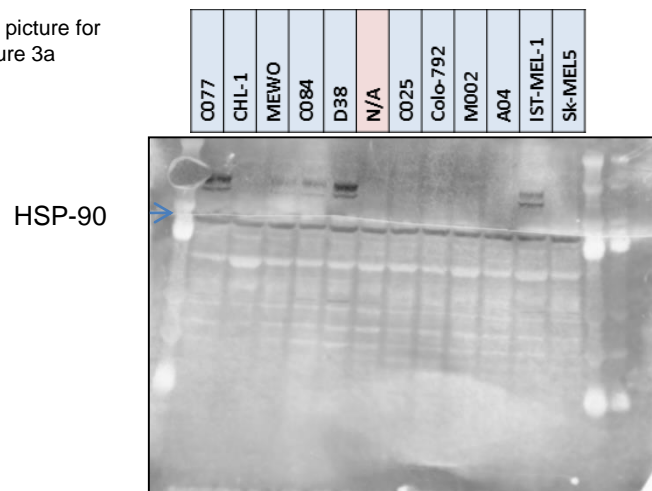
g



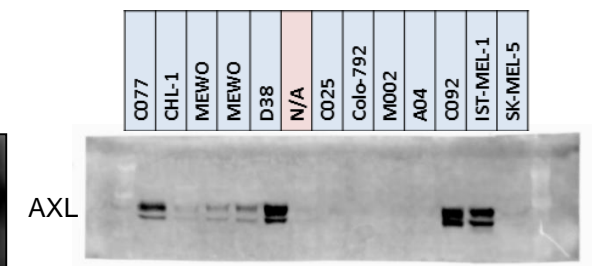
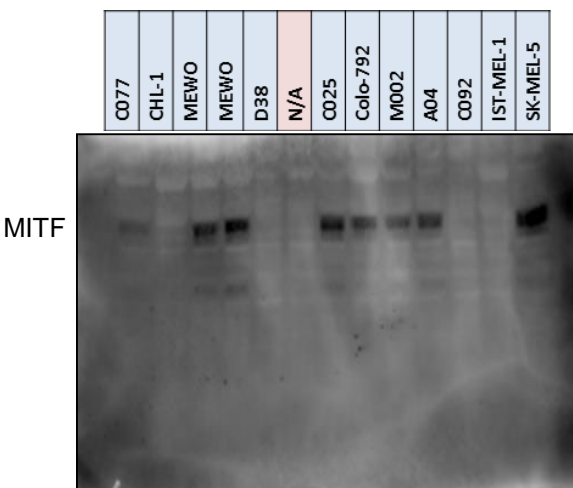
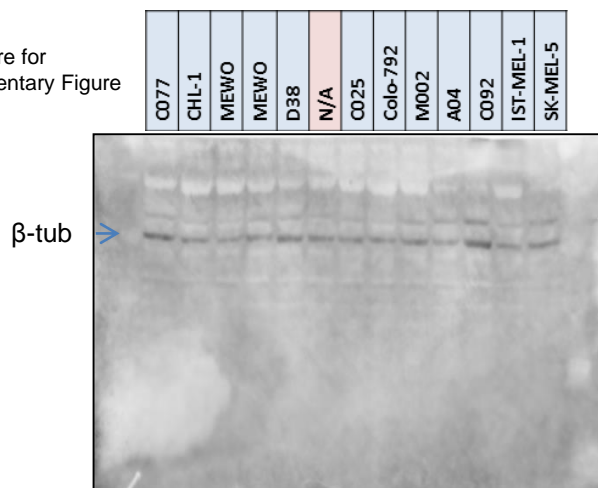
h



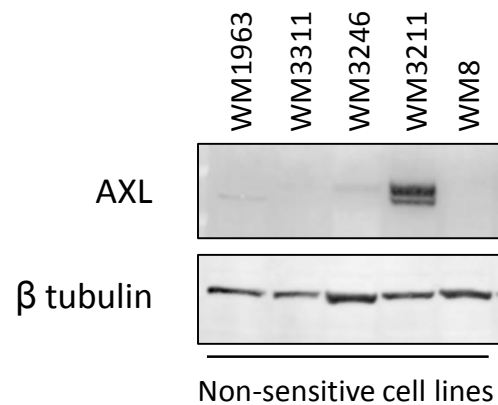
Full picture for Figure 3a



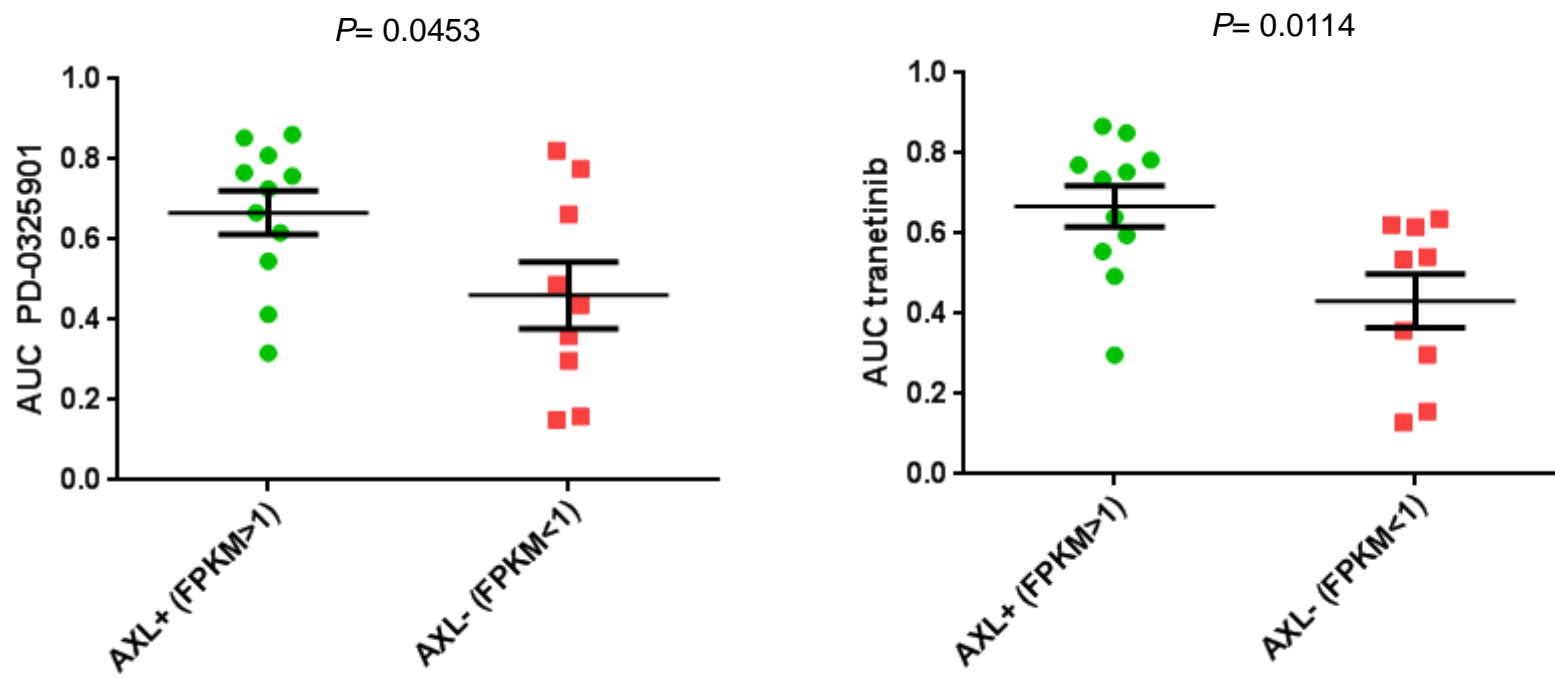
Full picture for Supplementary Figure 3h above



i



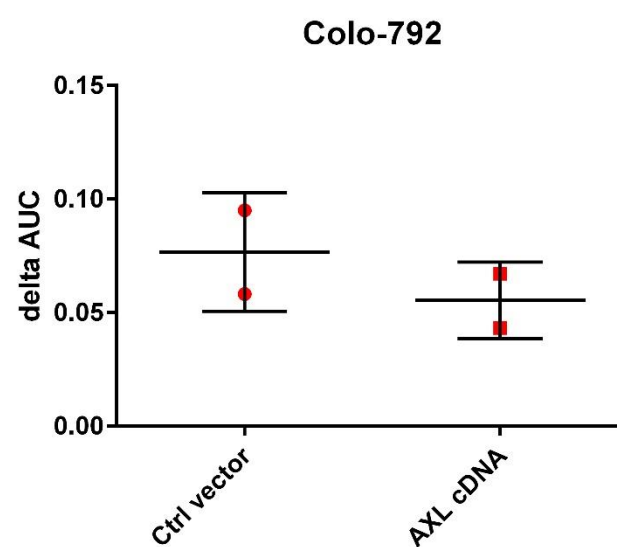
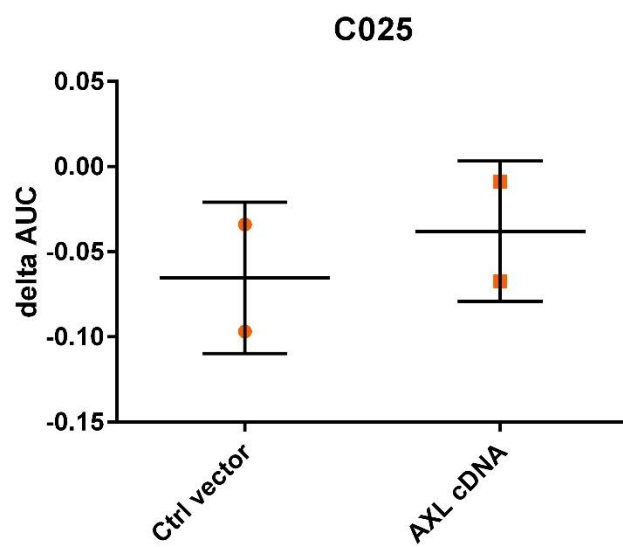
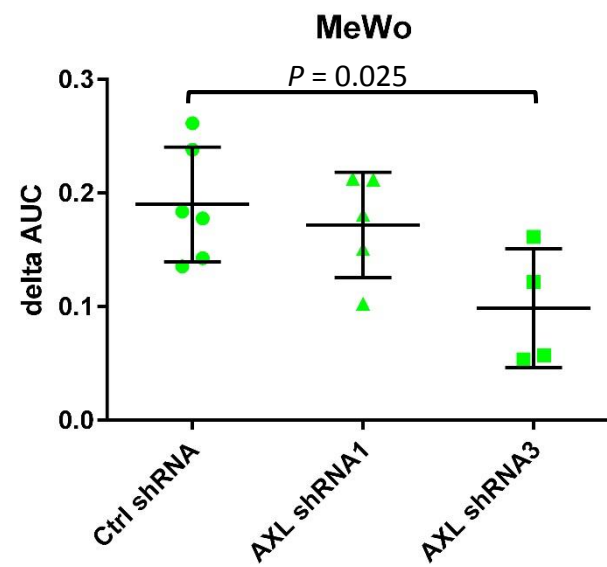
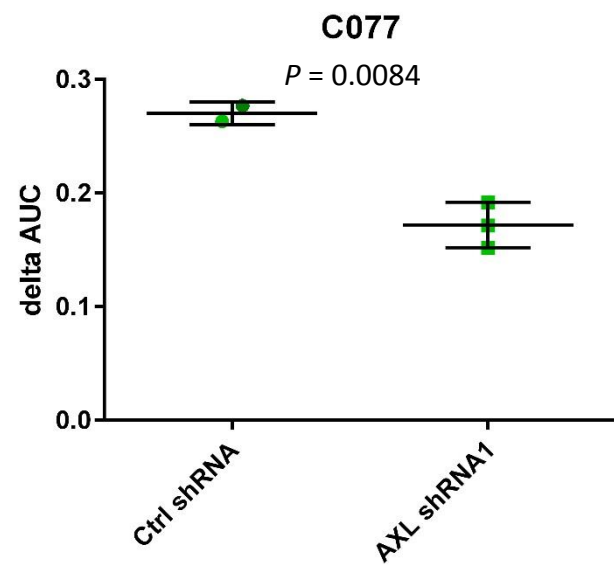
j





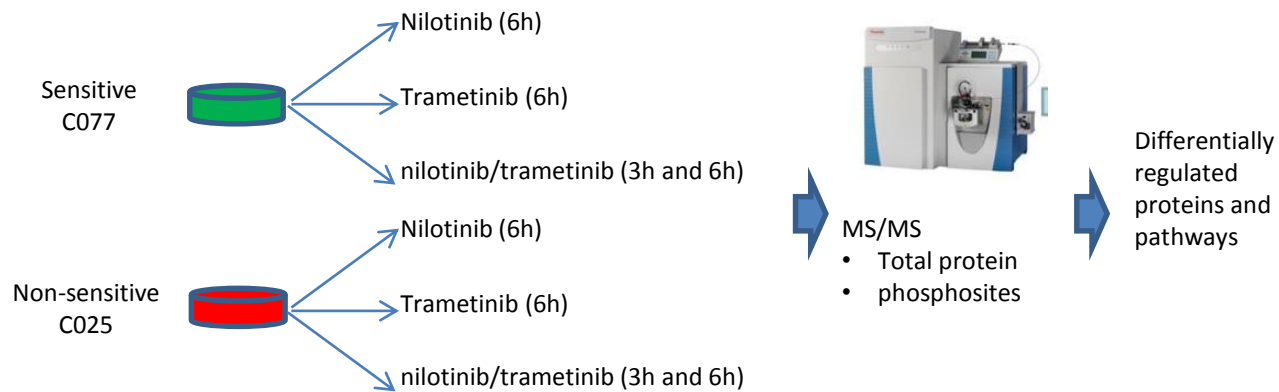


m

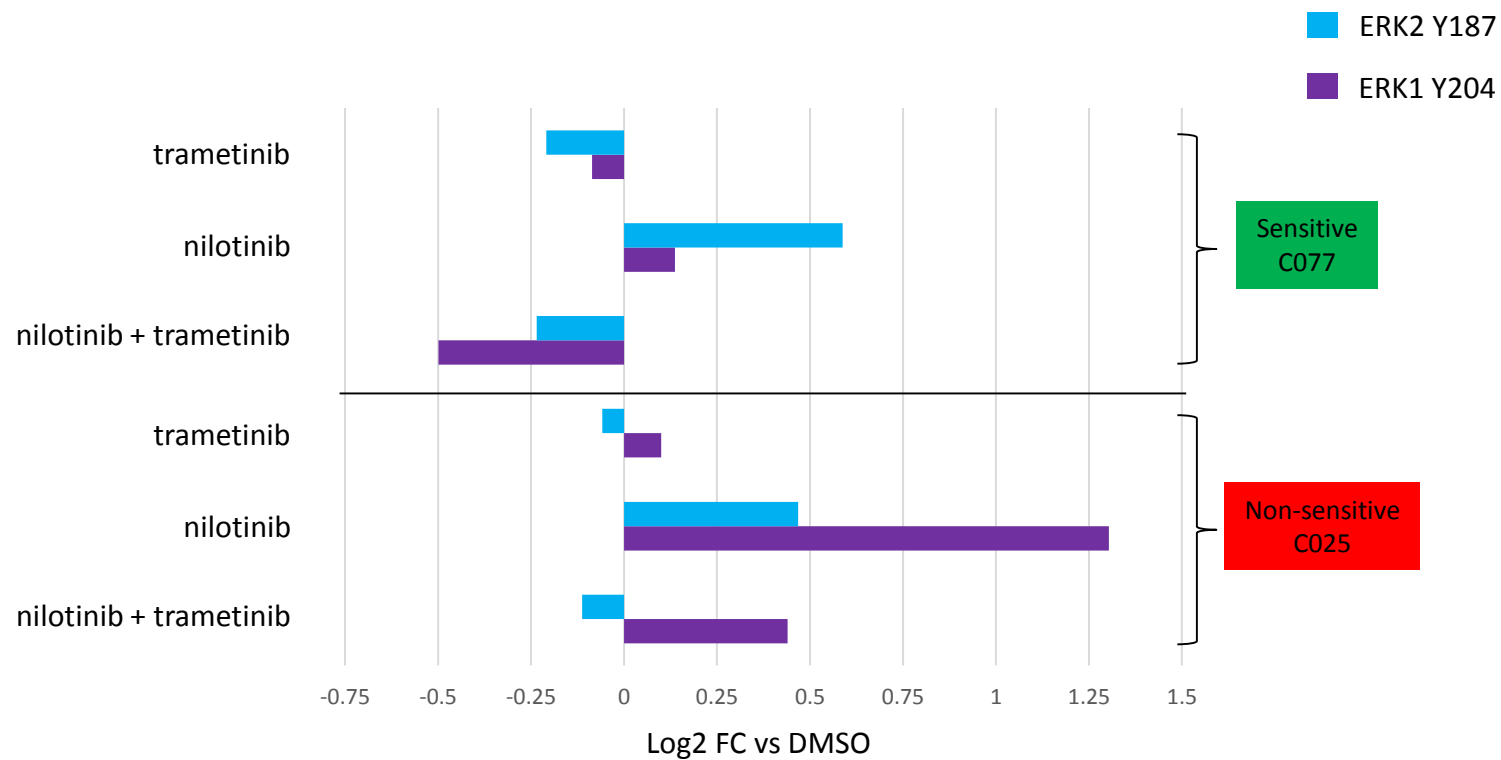


Supplementary Figure 3

n



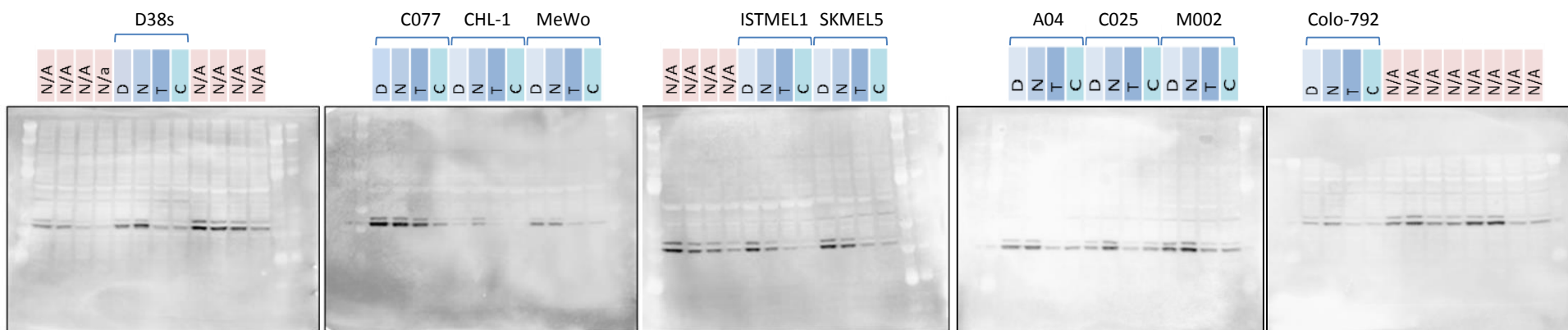
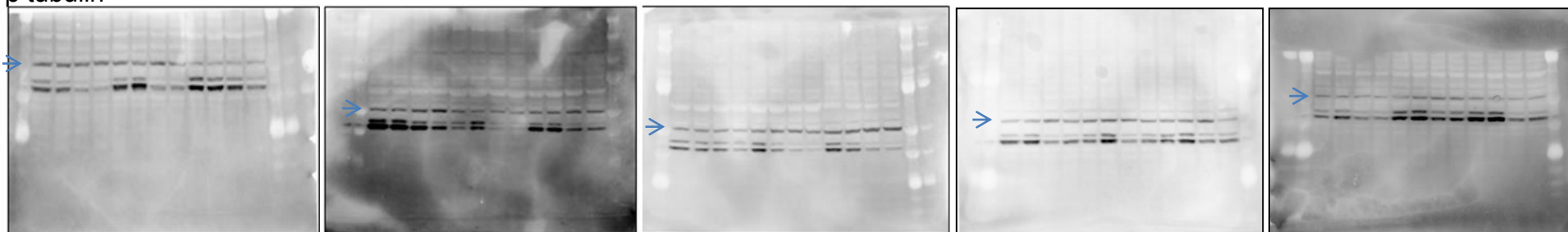
o



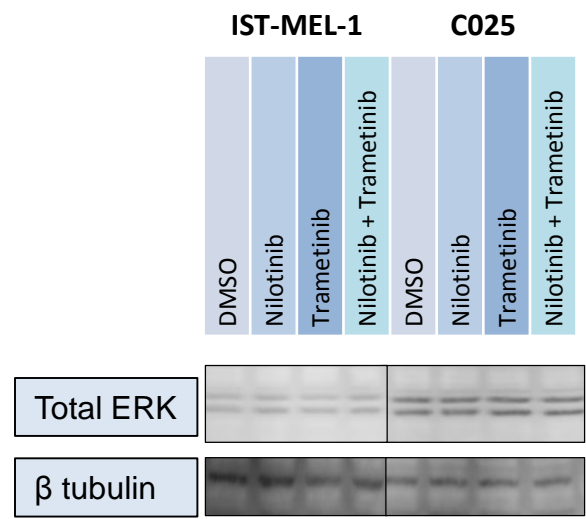
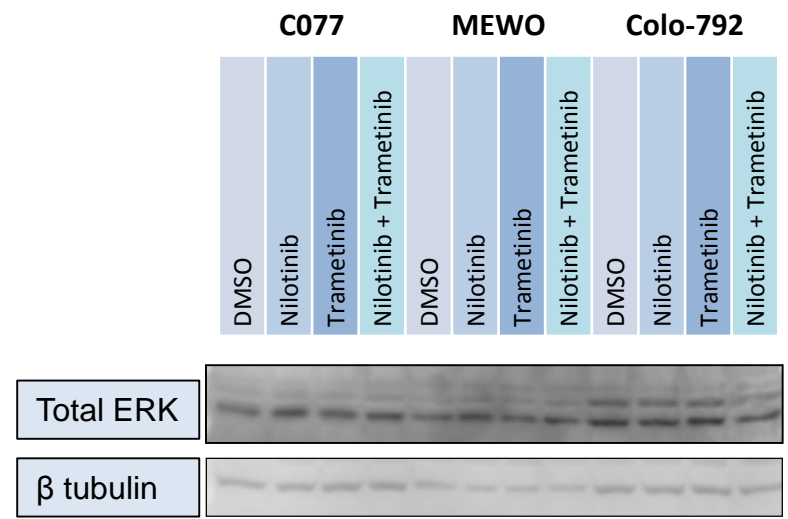
p

Full picture for Figure 3 b-c

p-ERK

 $\beta$  tubulin

q



### Supplementary Figure 3. Identification of the association between AXL expression and nilotinib/trametinib synergy.

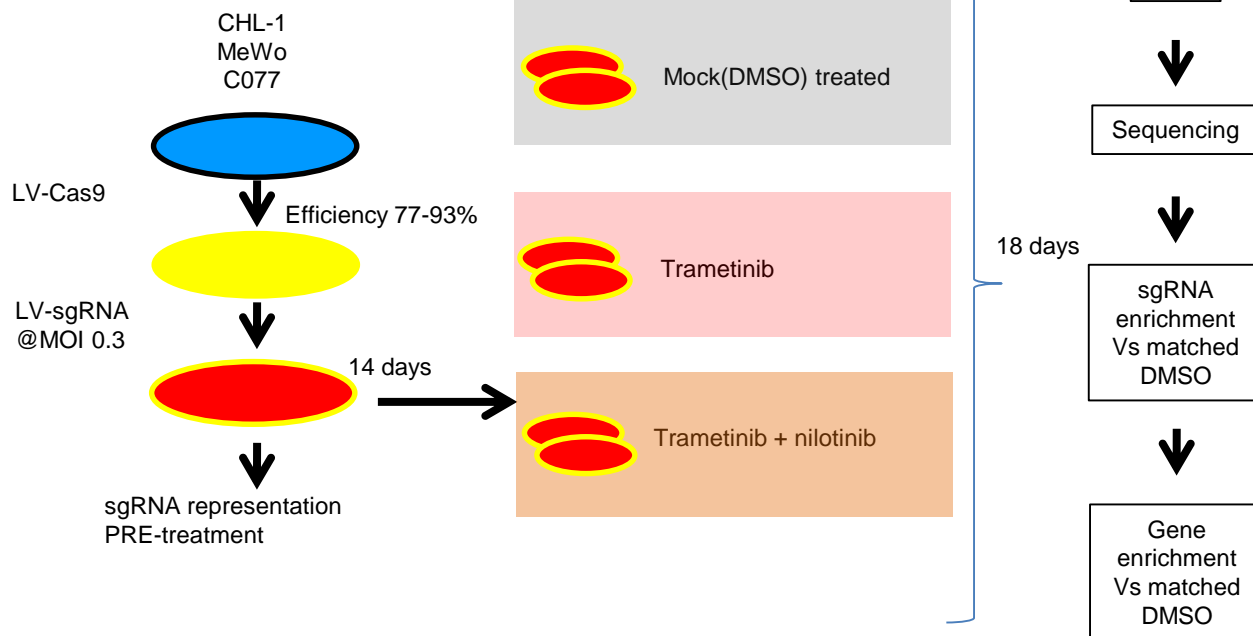
**a-b)** Pathway enrichment analysis for the genes up or downregulated, respectively, in sensitive vs non-sensitive cell lines. The enrichment analysis was run in MsigDB website considering Canonical Pathways and Hallmarks datasets. Minus  $\text{LOG}_{10}$  of the FDR corrected  $P$ -value is displayed in the histogram for the top 15 enriched pathways. **c-d)** Human tumors from Leeds (c) and TCGA (d) cohort that match the gene expression pattern associated with synergy or non-synergy and their classification into Jonsson's gene expression subclasses. The % of tumors significantly matching the gene expression pattern associated to synergy (synergy-like) or matching the opposite of the signature (non-synergy-like) are displayed in the histogram (see **Methods**). The total number (and %) of tumors classified as synergy-like and non-synergy-like in each cohort is indicated above the graph. The total number of tumors classified into each of the 4 Jonson classes (excluding the ones that failed to be classified into either synergy-like or non-synergy-like) is indicated on the left.  $P$ -value was calculated by two tailed Fisher's exact test comparing the number of synergy-like and non-synergy-like samples within a Jonsson's class vs the remaining 3 classes: \*  $P < 0.05$ , \*\*  $P < 0.01$ , \*\*\*  $P < 0.001$ , \*\*\*\*  $P < 0.0001$ . **e)** Expression (in FPKM) of *MITF* (X axis) and *AXL* (Y axis) in the *BRAF/NRAS* WT cell lines. Pearson correlation  $P$ -value, R squared and r values are indicated. **f-g)** Expression of *MITF* (f) and *AXL* (g) (in FPKM, Y axis) in the cell lines that displayed synergy for nilotinib plus MEK inhibitors (sensitive) and in the cell lines that did not (non-sensitive).  $P$  value by unpaired Student's t-test. **h)** Top panel: Western blot for *AXL* (above) and *MITF* (below) in sensitive and non-sensitive cell lines (green and red background, respectively; "intermediate" C092 cell line in yellow background). \*=*NRAS*<sup>Q61R</sup>-mutant cell line, ^=*BRAF*<sup>V600E</sup>-mutant cell lines.  $\beta$ -tubulin is shown as loading control. The eight samples on the left are biological replicates of the ones presented in Figure 3a. The black line separates different membranes. Bottom panels: Full pictures of western blot membranes presented in Fig.3a and above in the top panel. **i)** Western blot for *AXL* in the 5 *BRAF/NRAS* WT non-sensitive cell lines of the second melanoma collection.  $\beta$ -tubulin is shown as loading control. **j)** Sensitivity (expressed as AUC in Y axis) to PD-0325901 (left) and trametinib (right) in cell lines that express (FPKM>1, green), or not (FPKM<1, red) *AXL*.  $P$  value by unpaired Student's t-test, mean and standard error mean are shown. **k)** Western blot for *AXL* in sensitive cell lines transduced with lentiviral vectors expressing shRNA targeting *AXL* (left) and in non-sensitive cell lines transduced with a lentiviral vector expressing *AXL* cDNA (right).  $\beta$  tubulin is shown as loading control, volume of virus used for the infection is indicated in the legend. **l)** Survival curves of representative cell lines transduced with control vectors (top panels) or lentiviral vector expressing shRNA targeting *AXL* (left and middle bottom panel) or overexpressing *AXL* cDNA (right bottom panel). The Y axis shows viability vs vehicle treated control, X axis the concentration of trametinib (nM). The red line shows the viability of the cells treated with trametinib, the blue line the viability with nilotinib 2 $\mu$ M, the yellow line the viability with nilotinib/trametinib combination, the grey line the predicted additivity (see **Methods**). Each point is the average value of a technical triplicate. **m)** Delta AUC (Y axis) for nilotinib/trametinib combination in sensitive cell lines with knockdown of *AXL* (top panels) and in non-sensitive cell lines with *AXL* overexpression (bottom panels).  $P$ -values by unpaired Student's t-test; mean and standard error mean are shown. **n)** Experimental outline of the samples analysed for proteome and phosphoproteome. **o)** Variation of the detected ERK phosphopeptides (X axis, expressed as  $\log_2$  of the fold change vs DMSO-treated matched controls) in a sensitive (top part) and a non-sensitive (bottom part) cell line treated with trametinib (1nM), nilotinib (2 $\mu$ M) or nilotinib/trametinib

### Supplementary Figure 3

combination for 6 hours. The legend indicates the specific phosphorylation site. **p)** Full pictures of the membrane presented in Fig. 3b-c. N/A indicates samples not analysed for the scope of the manuscript. **q)** Western blot for total ERK upon treatment with DMSO vehicle, nilotinib (2 $\mu$ M), trametinib (1nM) or combination for 6h in representative cell lines.

# Supplementary Figure 4

a

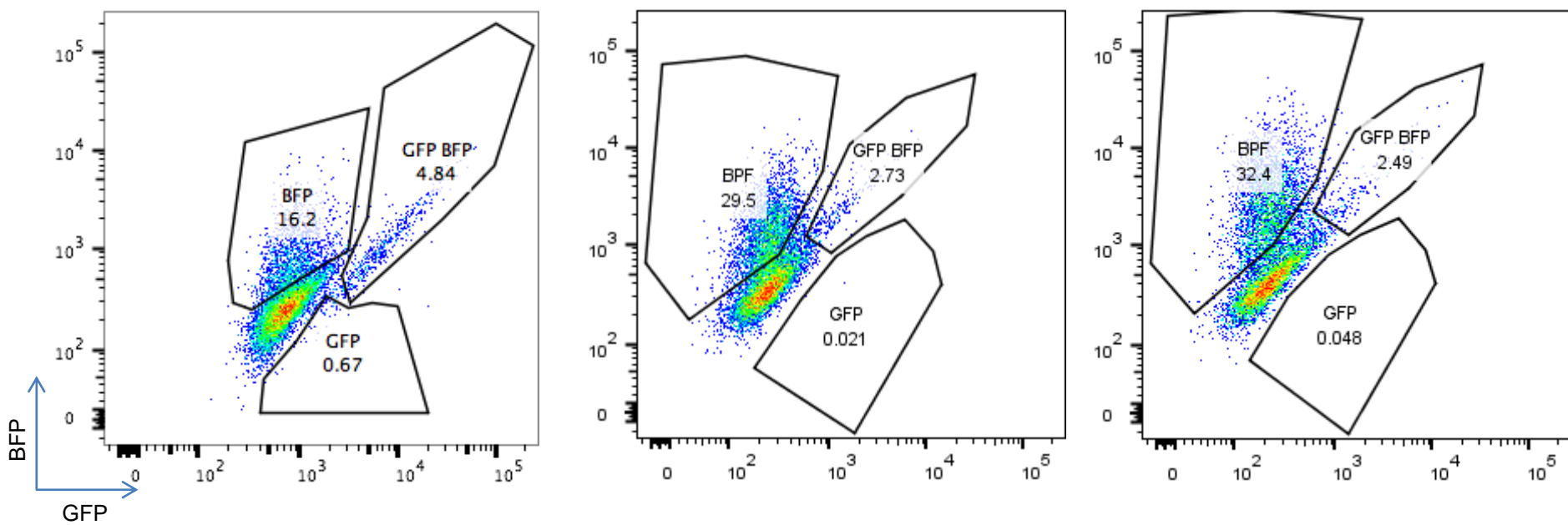


b

CHL-1 Cas9 activity: 77%

C077 Cas9 activity: 91.5%

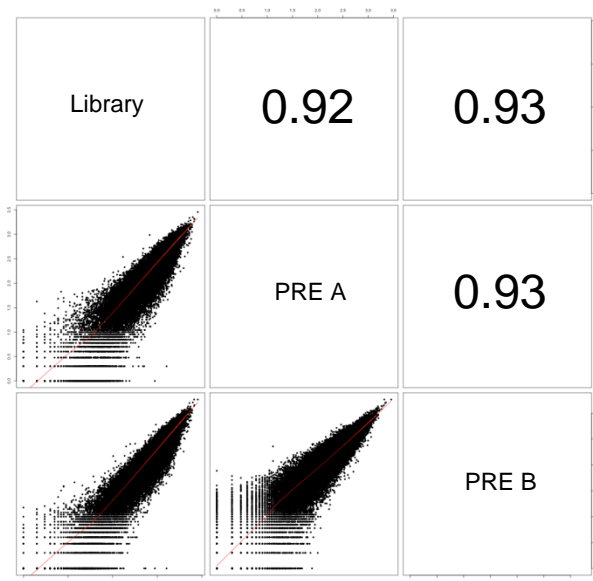
Mewo Cas9 activity: 92.9%



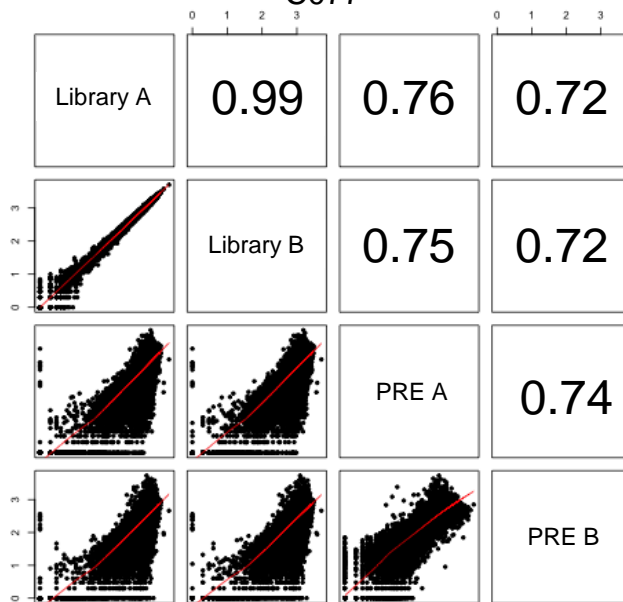
Supplementary Figure 4

c

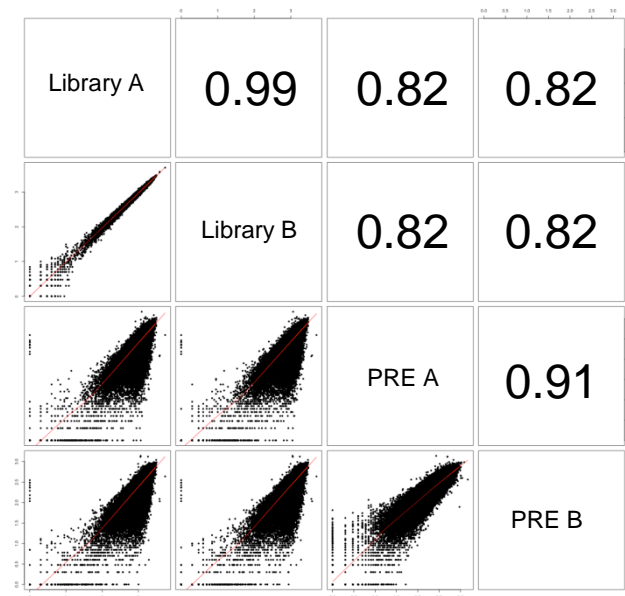
CHL-1



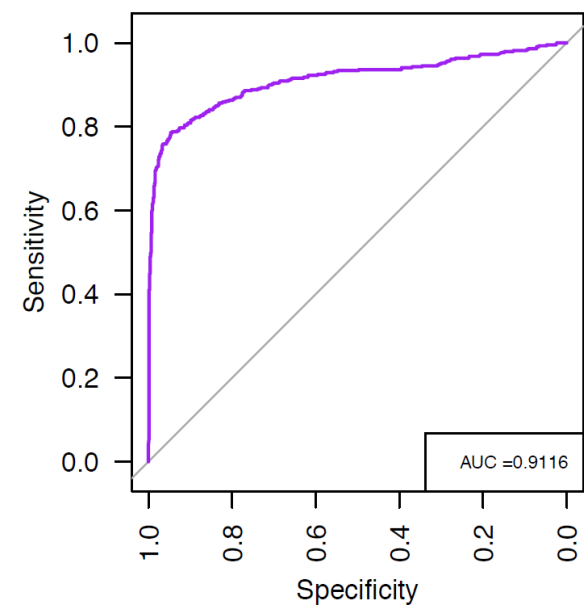
C077



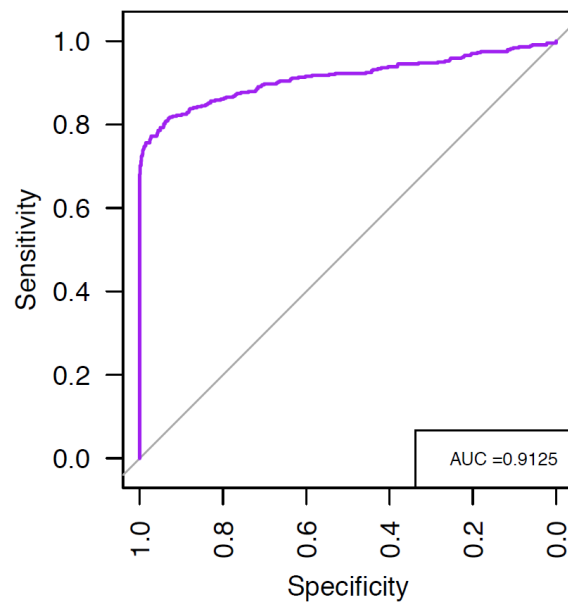
MeWo



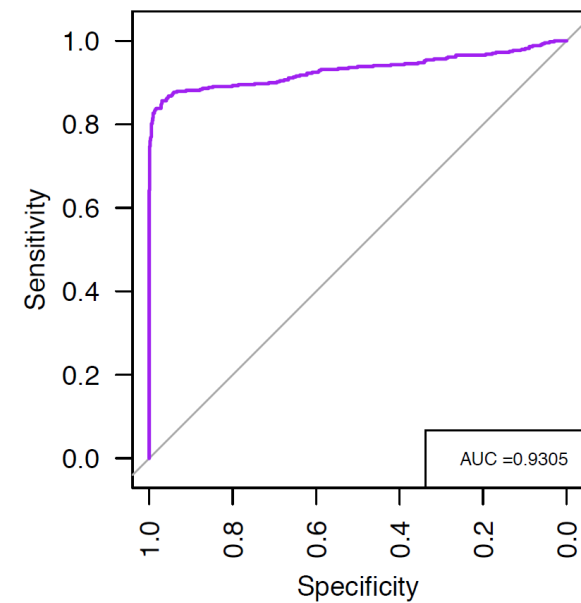
CHL1 PRE (A,B)



C077 PRE (A,B)



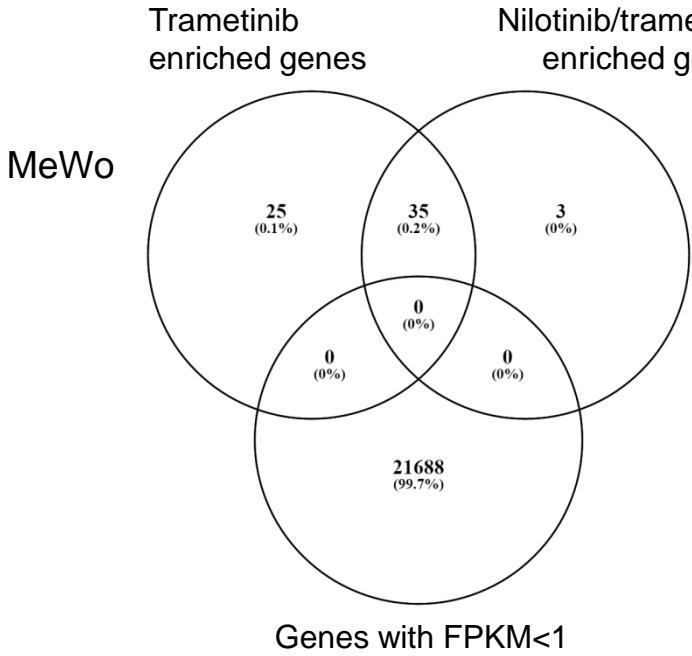
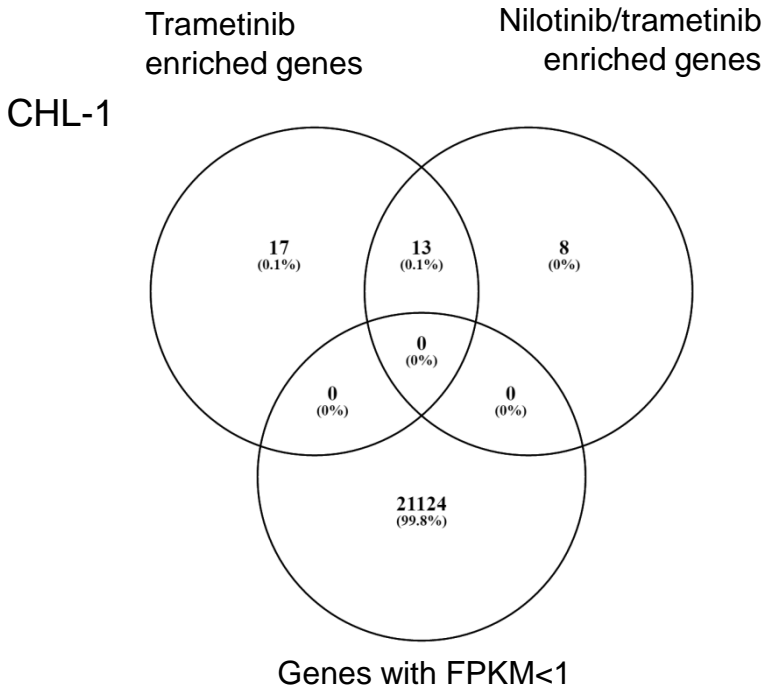
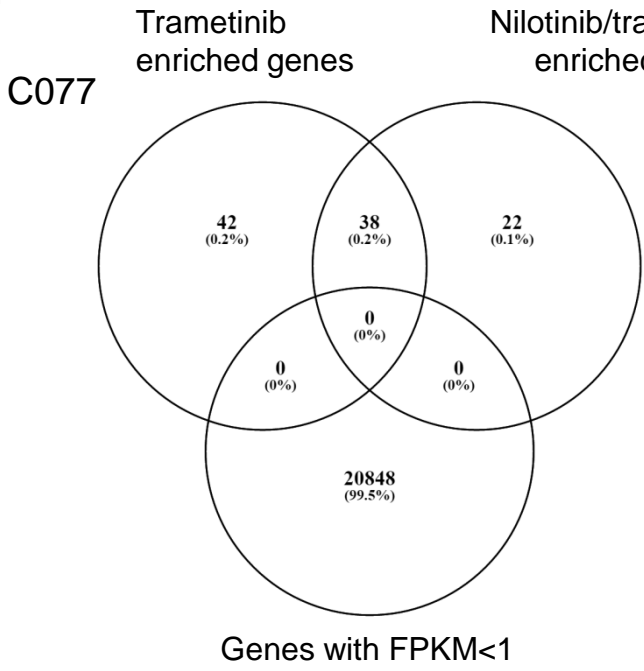
Mewo PRE (A,B)





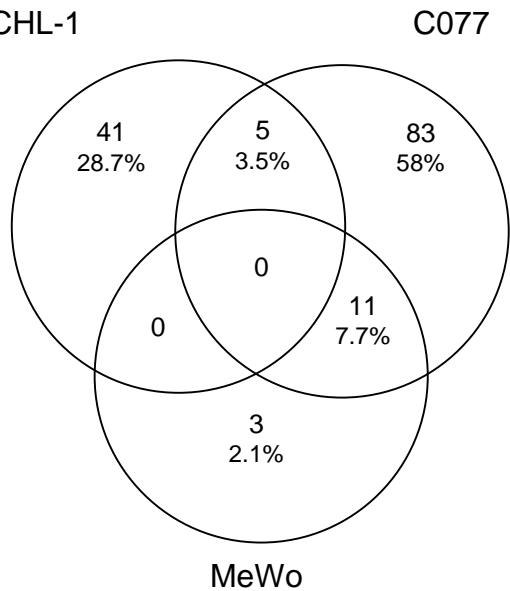
Supplementary Figure 4

d



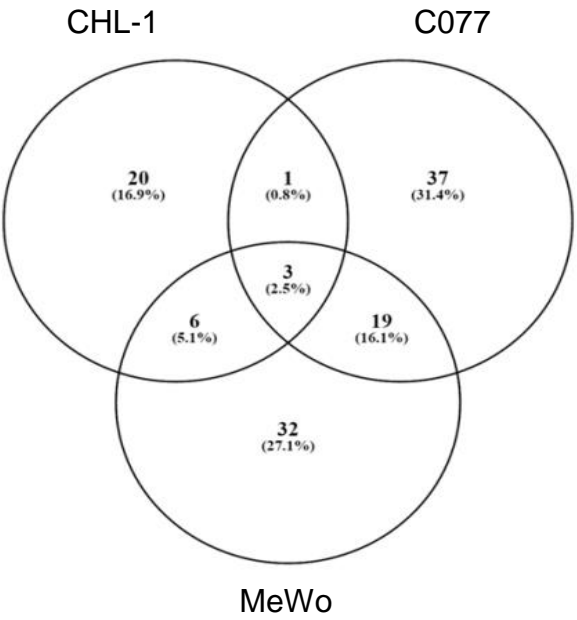
e

Pathway enriched in combination resistance genes



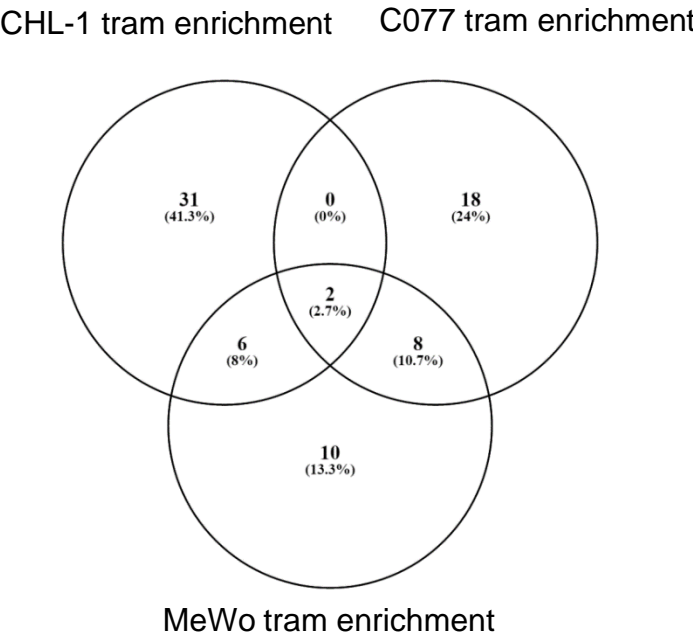
f

Trametinib resistance genes



g

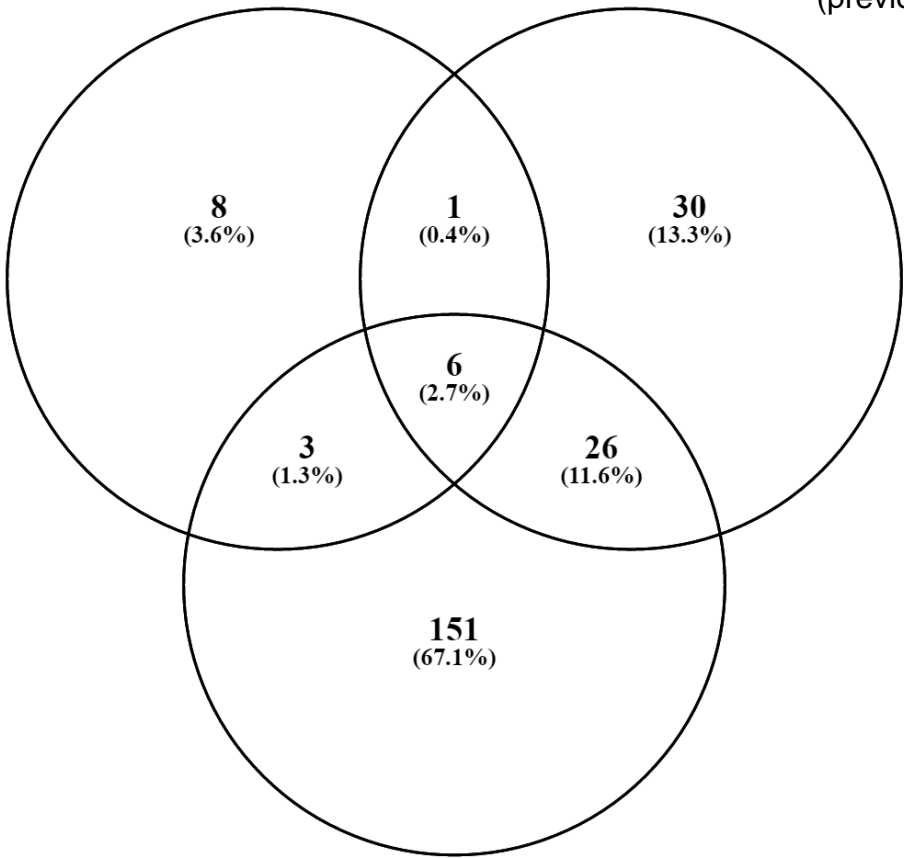
Pathway enriched in trametinib resistance genes



h

Nilotinib/trametinib resistance  
(our screen)

vemurafenib resistance  
(previous screens)



Selumetinib resistance  
(previous screens)

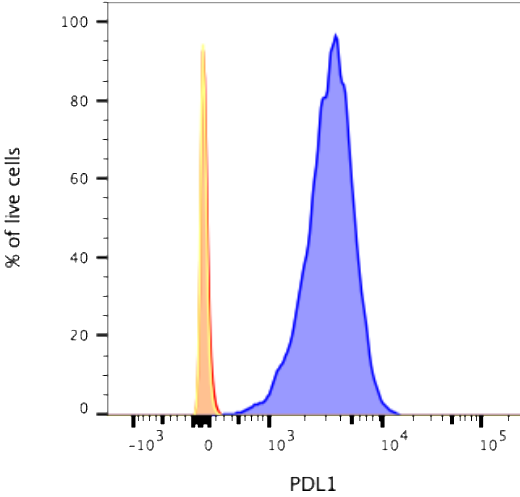


**Supplementary Figure 4. Identification of trametinib and nilotinib/trametinib drug resistance genes by CRISPR/Cas9 genome wide library screening.**

**a)** Experimental outline of the CRISPR/Cas9 screening. Briefly, we generated for each of the 3 cell lines a derivative that expresses efficiently Cas9 and transduced it in duplicate with the sgRNA library. Fourteen days after the library infection, we performed drug selection for each replicate with vehicle, trametinib or nilotinib/trametinib combination and collected them after 18 days of drug treatment to estimate by PCR and sequencing the representation of each sgRNA. **b)** Efficiency of the Cas9 cut in BFP/GFP reporter assay. The cells that stably express Cas9 were infected with a lentiviral vector (LV) that express BFP, GFP and a sgRNA targeting GFP (see **Methods**). BFP and GFP fluorescent intensity by FACS analysis (Log scale) are displayed in X and Y axis, respectively. Above the graph the Cas9 activity (ratio between BFP<sup>pos</sup>GFP<sup>neg</sup> and total BFP<sup>pos</sup>) is indicated. The gates for the analysis were defined using negative and single fluorescent controls. **c)** Quality control of the Cas9 screening experiment. The top panels show pair-wise Pearson correlation coefficients (upper right quadrants) and scatter plots (lower left quadrants) between sgRNA counts in replicates of infection prior to drug treatment (PRE A and B, 2 weeks after the library infection), and between each individual replicate and the reference counts from the plasmid library (2 replicate of sequencing for the library plasmid for C077 and MeWo). The bottom panel show receiver operating characteristic (ROC) curves quantifying classification performances of the gene essentiality scores derived applying MAGeCK to the pooled PRE A and B population vs the library. Two *a priori* defined gene sets of known essential and non-essential genes (as specified in the **Methods**) were considered as positive and negative cases, respectively. The performances assessment was restricted only to genes in these two sets. One plot per cell line is shown and the inset contains the extent of the area under each curve. Grey diagonal lines indicate performance expectations. **d)** Venn diagram among the Cas9 screening hits (FDR<0.1 in both duplicates) for trametinib, trametinib plus nilotinib, and poorly expressed genes (FPKM<1) for C077 (top left), CHL-1 (top right) and MeWo (bottom) cell lines. All the significant hits are expressed genes. **e)** Venn diagram of the significantly enriched pathways in the list of combination resistance genes for each cell line. The enrichment was performed on genes with FDR<0.1 in both replicates (see **Methods**). **f)** Venn diagram of the trametinib resistance genes (FDR<0.1 in both duplicates) among the 3 cell lines. **g)** Venn diagram of the significantly enriched pathways in the list of trametinib resistance genes for each cell line. The enrichment analysis was performed as in (e). **h)** Venn diagram showing the overlap between combination resistance genes identified in our screenings and vemurafenib and selumetinib resistance genes identified previously (see **Methods**). **i)** Status of the nilotinib/trametinib resistance genes in 4 collections of human tumors (by cBioportal, see **Methods**). Left panel: frequency of tumors carrying a mutation (red amplification, blue deep deletion, green missense mutation, grey multiple mutation type) in one of the 18 nilotinib/trametinib resistance genes. Top right panel: mutation status of the combination resistance genes in each of the melanoma from the TCGA cohort (n=287 samples analysed by cBioportal website); bottom right panel: mutation status of the combination resistance genes in melanoma from the Broad cohort (n=121 samples by cBioportal website). Each grey square represents a sample; only tumors with a mutation in the interrogated genes were displayed; frequency of mutation across the cohort per each gene is displayed on the right. Amplification/deletion data are available only for the TCGA cohort.

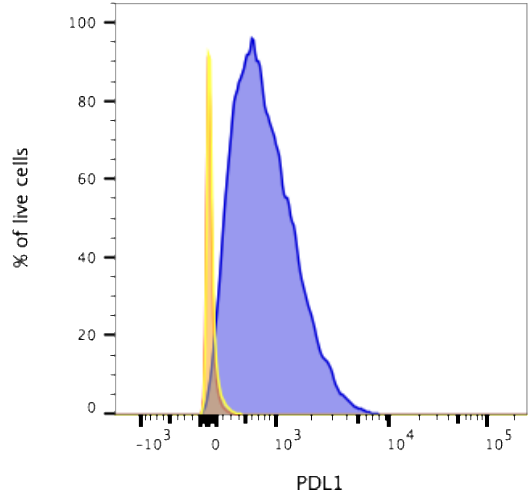
# Sensitive cell lines

CHL-1



Sample Name	% PDL1 positive
Nilotinib + Trametinib	0.071
IFNg (pos ctrl)	99.9
DMSO (neg ctrl)	0.14

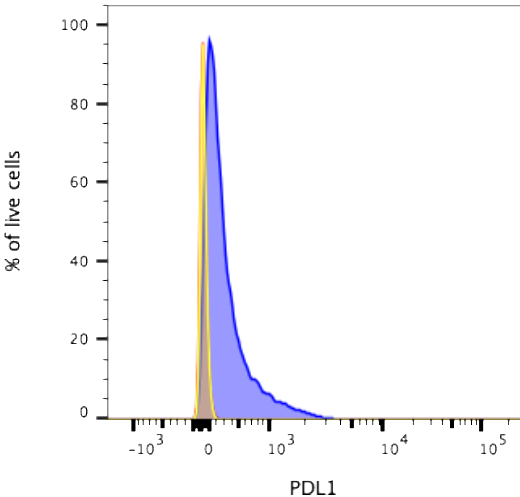
C077



Sample Name	% PDL1 positive
Nilotinib + Trametinib	3.63
IFNg (pos ctrl)	93.5
DMSO (neg ctrl)	2.13

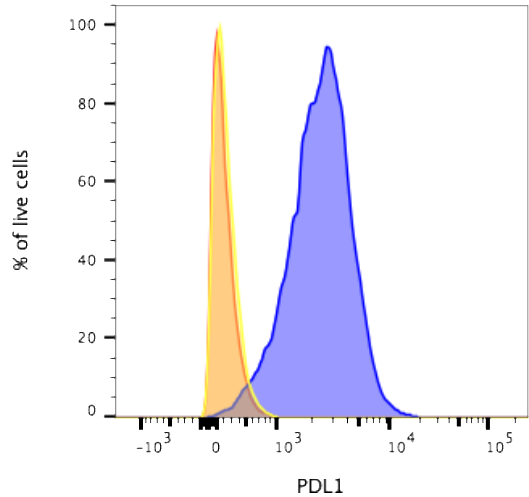
# Non-sensitive cell lines

Colo-792



Sample Name	% PDL1 positive
Nilotinib + Trametinib	0.38
IFNg (pos ctrl)	61.0
DMSO (neg ctrl)	0.59

C025



Sample Name	% PDL1 positive
Nilotinib + Trametinib	2.35
IFNg (pos ctrl)	97.1
DMSO (neg ctrl)	1.91

## Supplementary Figure 5

### **Supplementary Figure 5. The nilotinib/trametinib combination treatment did not induce PD-L1 expression in *BRAF/NRAS* WT melanoma cell lines.**

PD-L1 expression by flow cytometry, shown as % of live cells (Y axis), in 2 sensitive (top panel) and 2 non-sensitive (bottom panel) cell lines. Cells were treated for 72h with DMSO (vehicle, in red), 50ng/ml IFN $\gamma$  (positive control of PD-L1 induction, in blue) or 2 $\mu$ M nilotinib + 1nM trametinib (drug combination, in yellow). PD-L1 expression of all cell lines was induced by IFN $\gamma$  treatment, however treatment with the nilotinib/trametinib combination did not alter the PD-L1 expression of any of the cell lines.